Electronic Supplementary Material (ESI) for Nanoscale.


# Fabrication of Graphene Layer Probe to Measure Force Interactions in Layered Heterojunctions

*Jianfeng Li,*[a] *Jinjin Li,*,*[a] *Liang Jiang,*[b] *and Jianbin Luo*[a]

[a] *State Key Laboratory of Tribology, Tsinghua University, Beijing 100084, China.*

[b] *Tribology Research Institute, State Key Laboratory of Traction Power, Southwest Jiaotong University, Chengdu 610031, China.*

1. An optical microscope image of multilayer graphene nanoflakes on a glass slide

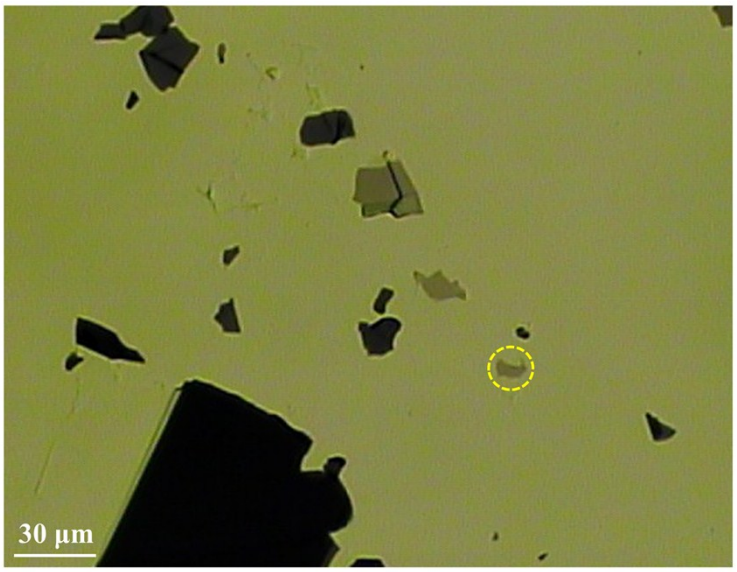


**Figure S1** Optical microscope image of many multilayer graphene nanoflakes on a clean glass slide, which were exfoliated from the flake graphite using Scotch tape. The yellow circle highlights a multilayer graphene nanoflake with a size of around 10 × 10

μm$^2$ and a thickness of approximately 1–30 nm, which was suitable for fabricating a graphene layer probe.

2. The friction coefficients between six graphene layer probes and HOPG

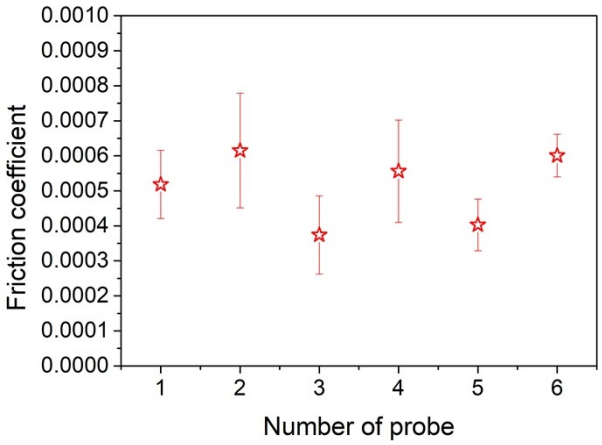


**Figure S2** The friction coefficients between six graphene layer probes and HOPG. The test parameters were the same as that of the friction measurement shown in Figure 2a.

3. FESEM image and Raman spectrum of the graphene layer probe after sliding a long distance

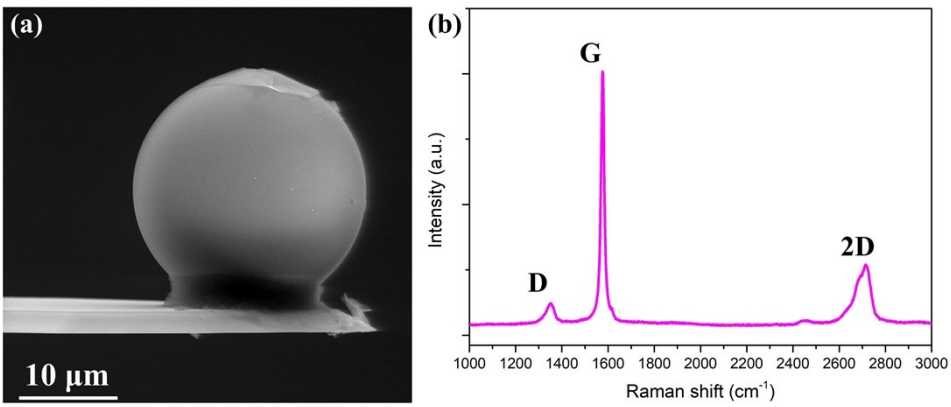


**Figure S3** (a) FESEM image of the graphene layer probe after sliding a long distance. (b) Raman spectrum of the graphene layer probe after sliding a long distance.

4. The frictional forces and adhesive forces between the graphene layer probe and HOPG under different relative humidities.

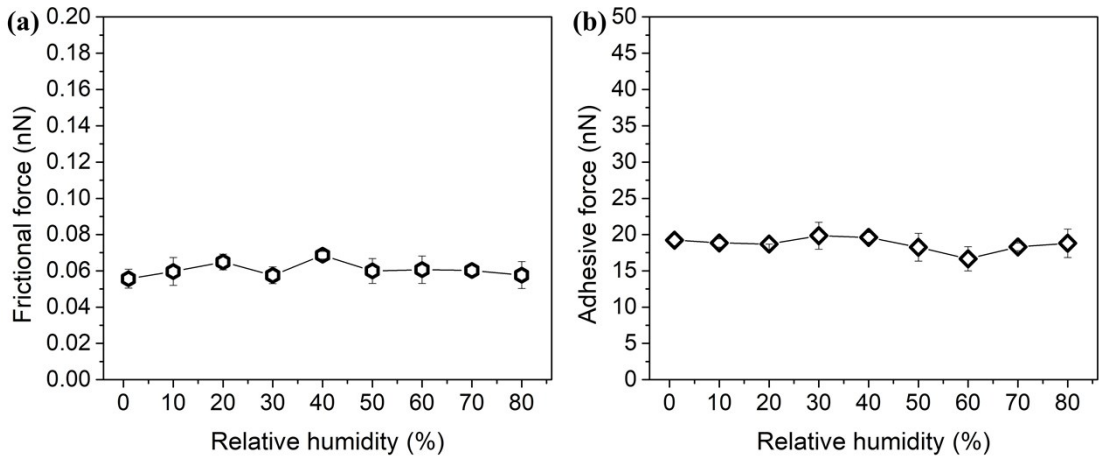


**Figure S4** (a) The frictional forces between the graphene layer probe and HOPG under different relative humidities. The relative humidity ranged from 0% to 80% (0% corresponds to dry nitrogen atmosphere). The normal load was 36 nN and the sliding velocity was 4 μm/s. The frictional forces under different relative humidities maintained approximately 0.06 nN. (b) The adhesive forces between the graphene layer probe and HOPG under different relative humidities. The relative humidity ranged from 0% to 80% (0% corresponds to dry nitrogen atmosphere) and the approach/retract velocity of the probe was 500 nm/s. The adhesive forces under different relative humidities maintained approximately 19 nN.

5. Typical normal forces as functions of separation of the four layered heterojunctions

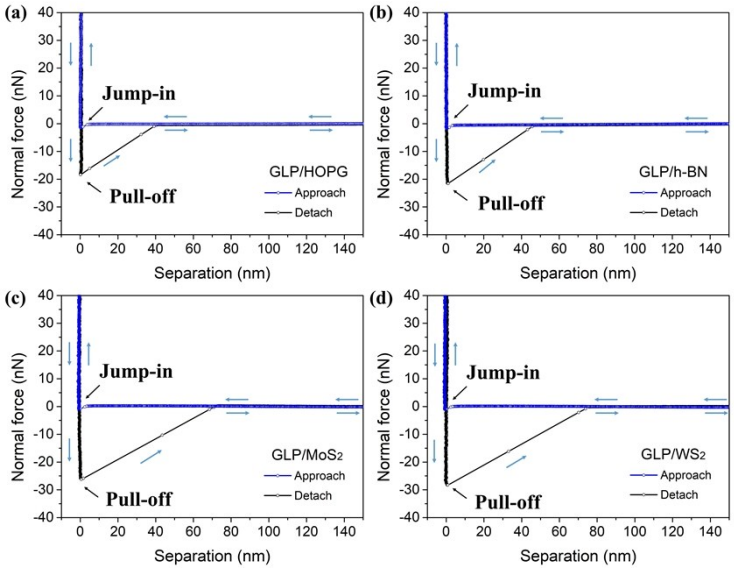


**Figure S5** Normal forces as functions of separation when the graphene layer probe approached the topmost layers of four 2D layered materials and then detached from them. The approach/retract velocity of the probe was 500 nm/s.

6. Adhesive force maps of the four layered heterojunctions in 1000 × 1000 $nm^2$ area

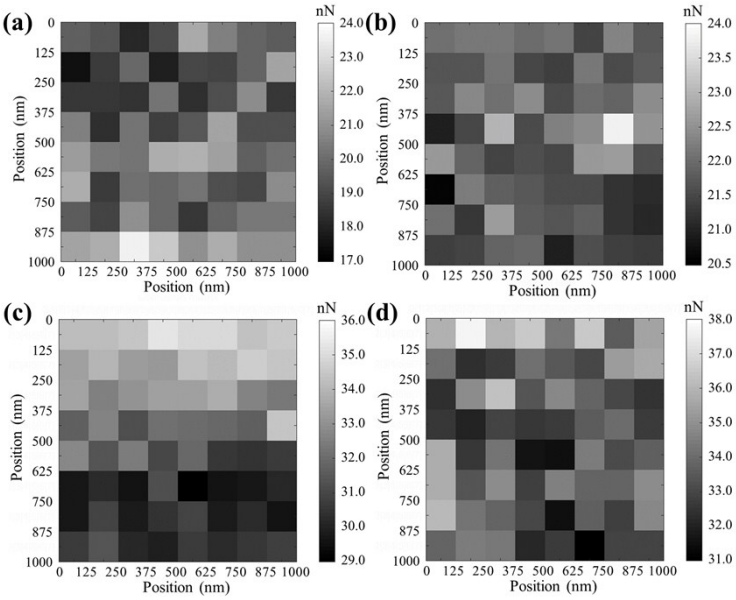

**Figure S6** Adhesive force maps extracted from 64 normal force curves in an area of 1000 × 1000 $nm^2$ when the graphene layer probe first approached the four 2D layered materials and subsequently detached from them: (a) GLP/HOPG, (b) GLP/h-BN, (c) GLP/$MoS_2$, and (d) GLP/$WS_2$.

7. Explanation of multi-asperity contact between the graphene layer probe and HOPG

The topography on the top region of the graphene layer probe was investigated by AFM by driving a silicon tip array with a period of 3 μm to slide against the graphene layer probe, as shown in Figure S7a. Asperities on the surface were observed, and the root mean square roughness over the whole area was calculated to be about 1 nm. Based on the cross-sectional height profile (Figure S7b), the distance between two adjacent asperities was about 20 nm. Therefore, the surface of the graphene layer probe was not atomically flat, and it was inferred that the graphene layer probe formed multi-asperity contact with the HOPG.

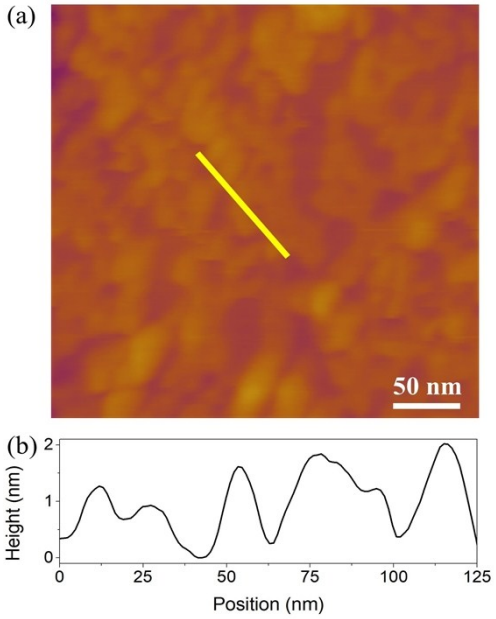

**Figure S7** (a) AFM image of the topography on the top central region of the graphene layer probe with a scanning area of 300 × 300 $nm^2$ using tapping mode. (b) Cross-sectional height profile of the graphene layer probe surface along the yellow line in (a).

8. Physical parameters of the four 2D layered materials and air

**Table S1** Physical parameters of the four 2D layered materials and air

| | Graphene (HOPG) | h-BN | $MoS_2$ | $WS_2$ | Air |
|---|---|---|---|---|---|
| Interlayer shear stress (MPa) | 0.25–0.75[1] | 0.3[2] | 16–17[3] | 20.0[4] | |
| Static dielectric constant | 5.0[5] | 4.0[6] | 12.8[7] | 11.5[7] | 1 |
| Refractive index | 1.93[8] | 1.85[9] | 3.97[7] | 3.58[7] | 1 |
| Surface energy ($mJ/m^2$) | 70–110[10,11] | 110[12] | 250–260[13-15] | 250–260[13-15] | |

9. Calculated Hamaker constants of the four layered heterojunctions

**Table S2** Calculated Hamaker constants of the four layered heterojunctions

| | GLP/HOPG | GLP/h-BN | GLP/$MoS_2$ | GLP/$WS_2$ |
|---|---|---|---|---|
| Calculated Hamaker constant ($10^{-19}$J) | 1.91 | 1.78 | 3.80 | 3.57 |

## References

(1) Soule, D. E.; Nezbeda, C. W., Direct basal-plane shear in single-crystal graphite. *Journal of applied physics* **1968,** *39* (11), 5122-5139.

(2) Androulidakis, C.; Koukaras, E. N.; Poss, M.; Papagelis, K.; Galiotis, C.; Tawfick, S., Strained hexagonal boron nitride: Phonon shift and Grüneisen parameter. *Physical Review B* **2018,** *97* (24), 241414.

(3) Briscoe, B. J.; Smith, A. C., The interfacial shear strength of molybdenum disulfide and graphite films. *ASLE TRANSACTIONS* **1982,** *25* (3), 349-354.

(4) Lian, Y.; Deng, J.; Yan, G.; Cheng, H.; Zhao, J., Preparation of tungsten disulfide ($WS_2$) soft-coated nano-textured self-lubricating tool and its cutting performance. *The International Journal of Advanced Manufacturing Technology* **2013,** *68* (9-12), 2033-2042.

(5) Wang, X.-F.; Chakraborty, T., Collective excitations of Dirac electrons in a graphene layer with spin-orbit interactions. *Physical Review B* **2007,** *75* (3).

(6) Chiang, T. H.; Hsieh, T. E., A study of encapsulation resin containing hexagonal boron nitride (hBN) as inorganic filler. *Journal of Inorganic and Organometallic Polymers and Materials* **2006,** *16* (2), 175-183.

(7) Kumar, A.; Ahluwalia, P. K., Tunable dielectric response of transition metals dichalcogenides $MX_2$ (M=Mo, W; X=S, Se, Te): Effect of quantum confinement. *Physica B-Condensed Matter* **2012,** *407* (24), 4627-4634.

(8) Zhang, W.; Zhou, M.; Amoako, G.; Shao, Y. L.; Li, B. J.; Li, J.; Gao, C. Y., Formation of Laser-induced Periodic Surface Structures During Femtosecond Laser Ablation of Highly Oriented Pyrolytic GLPphite (HOPG). *Lasers in Engineering* **2013,** *25* (5-6), 397-404.

(9) Golla, D.; Chattrakun, K.; Watanabe, K.; Taniguchi, T.; LeRoy, B. J.; Sandhu, A., Optical thickness determination of hexagonal boron nitride flakes. *Applied Physics Letters* **2013,** *102* (16).

(10) Hernandez, Y.; Nicolosi, V.; Lotya, M.; Blighe, F. M.; Sun, Z.; De, S.; McGovern, I. T.; Holland, B.; Byrne, M.; Gun'Ko, Y. K., High-yield production of graphene by liquid-phase exfoliation of graphite. *Nature nanotechnology* **2008**, *3* (9), 563.

(11) H.O. Pierson, Handbook of Carbon, Graphite, Diamond, and Fullerenes: Properties, Processing, and Applications, Noyes, Park Ridge, NJ, **1993**.

(12) Knowles, K. M.; Turan, S., High Resolution Transmission Electron Microscopy of Grain Boundaries between Hexagonal Boron Nitride Grains in Si3N4—SiC Particulate Composites. *Crystal Research and Technology: Journal of Experimental and Industrial Crystallography* **2000**, *35* (6-7), 751-758.

(13) Weiss, K.; Phillips, J. M., Calculated specific surface energy of molybdenite ($MoS_2$). *Physical Review B* **1976**, *14* (12), 5392.

(14) Shang, S.-L.; Lindwall, G.; Wang, Y.; Redwing, J. M.; Anderson, T.; Liu, Z.-K., Lateral versus vertical growth of two-dimensional layered transition-metal dichalcogenides: thermodynamic insight into MoS2. *Nano letters* **2016**, *16* (9), 5742-5750.

(15) Chen, X.; Boulos, R. A.; Eggers, P. K.; Raston, C. L., p-Phosphonic acid calix [8] arene assisted exfoliation and stabilization of 2D materials in water. *Chemical Communications* **2012**, *48* (93), 11407-11409.